Numerical Investigation of Energy Absorption in Dual Metal Hydride Bed based Thermo-Chemical Energy Storage System

Sumeet Kumar Dubey[1], K. Ravi Kumar[1], Vinay Tiwari[2] and Umish Srivastava[2]

[1] Department of Energy Science and Engineering, Indian Institute of Technology Delhi (India)

[2] Department of Solar Energy, Indian Oil Corporation (IOC) R&D Faridabad, Haryana (India)

Abstract

The analysis deals with the feasibility and performance study of a dual metal hydride bed system for thermal energy absorption at a higher temperature. An integrated dual bed system includes a metal hydride bed which acts as energy storage media operating at higher temperatures and another bed used as hydrogen storage media. $NaMgH_2F$ is used as high temperature metal hydride (HTMH), while Mg_2NiH_4 is used as low temperature metal hydride (LTMH). Study of the heat transfer phenomenon during thermal energy absorption in HTMH and hydrogen storage in low temperature metal hydride is performed. The variation of temperature, saturation fraction along with density variation of metal hydride bed is performed in this work.

Keywords: Concentrating solar power, High temperature thermal energy storage, Thermochemical energy storage, Dual metal hydride system.

1. Introduction

The decreasing reserves of fossil fuels and the effect on climate due to their combustion have forced masses to think about renewable energy sources. The high potential of solar energy to fulfill the energy demand with the objective of a clean and green environment makes solar energy favorable. Due to diurnal variation and the interrupted nature of solar energy, continuous power generation is one big challenge affecting the overall power generation capacity and unit cost of power generation. Integration of the energy storage system will help the power generation plant to operate for more hours, increasing the capacity of power generation and possibly bringing down the power generation cost.

Thermal energy storage (TES) systems are classified as sensible, latent, and thermochemical (Jain et al., 2021a). In a sensible storage system, the system stores energy by changing the temperature of the storage media, while the change of phase of storage media is responsible for thermal energy storage in the latent storage system. Thermochemical energy storage (TCES) systems store and release heat by carrying out endothermic and exothermic chemical reactions, respectively. The difference in thermal energy storage mechanisms can be understood clearly from figure 1.

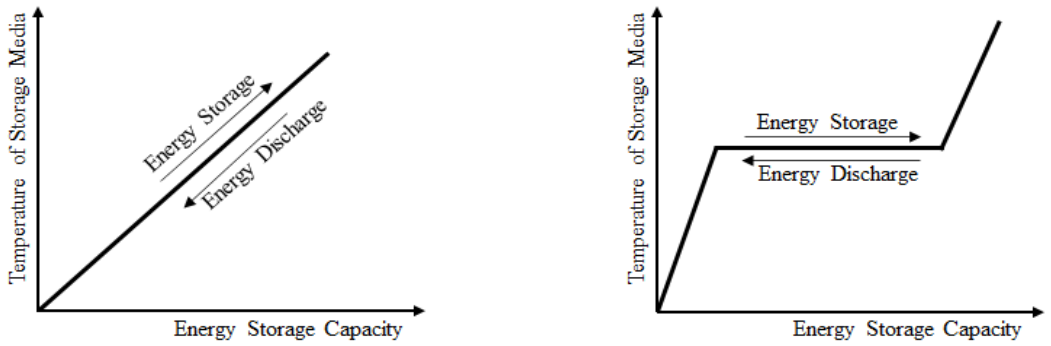

a) b)

doi:10.18086/eurosun.2022.13.07 Available at http://proceedings.ises.org

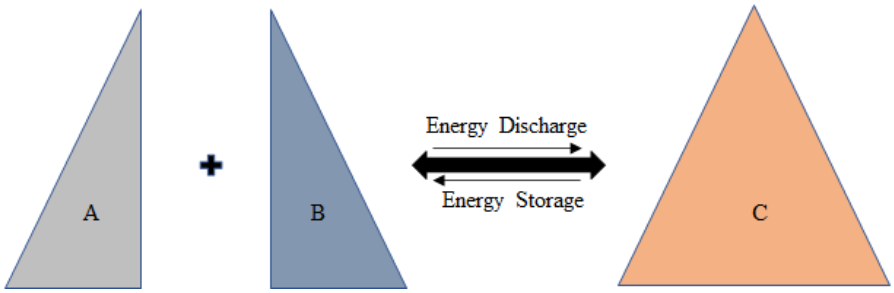

c)

Fig 1: Mechanism of thermal energy storage a) sensible, b) latent and c) thermochemical

Some metal alloys react with hydrogen and undergo an exothermic chemical reaction to form a metal hydride, which results in an energy discharge cycle, while during the endothermic chemical reaction, energy charging cycle takes place and metal hydride is dissociated into metal alloy and hydrogen.

Sensible energy storage technology is matured and commercially available for TES applications. The latest energy storage system has been studied, and several latent energy storage media are found appropriate for TES applications at higher temperature (Jain et al., 2021b; Ray et al., 2021). Several thermochemical energy storage systems have been reported suitable for high temperature TES applications (Chen et al., 2018; Choudhari et al., 2021; Liu et al., 2018; Møller et al., 2017; Pelay et al., 2017; Reilly and Wiswall, 1967; Sheppard et al., 2016b, 2016a; Sunku Prasad et al., 2019).

Metal hydride based TCES systems have been studied for TES applications. In earlier studies of metal hydride, Magnesium (Mg) alloys attracted researchers for thermal energy storage applications because of their higher thermal stability and reaction enthalpy. Mg based metal hydride was used for the application of steam generation application where the waste heat from the industries was stored in the Mg based hydride system and steam was produced by supplying thermal energy from Mg based hydride system. The system supplied heat at 370 ºC with a reported capacity of 9.08 kWh and 79.64% energy storage efficiency (Bogdanović et al., 1995). A small scale Mg hydride system used 19 gm of Mg hydride for analysis of energy absorption (Paskevicius et al., 2015). The study reported thermal energy storage at 420 ºC for 20 cycles with almost constant storage capacity. Due to the small capacity of the system, the heat losses were higher, but the author expected a reduction in heat losses with the increase in the capacity of the system. Nickel (Ni), cobalt (Co), and ferrous (Fe) were doped in Mg based hydride to study the variation in storage characteristics (Reiser et al., 2000a). With the addition of these elements, cyclic stability, reversibility, and operating temperature ranges of Mg hydride alloy have increased, while a slight reduction in thermal stability has been observed. Another study compared Ni doped Mg hydride with pure Mg hydride for hydrogen storage application, but the energy storage characteristics were also reported (Bogdanović et al., 1999). Authors reported improvement in cyclic stability, reversibility, and operating temperature range for Ni doped Mg hydride as compared to pure Mg hydride.

Numerical investigation of Magnesium Nickel (Mg-Ni) alloy aimed to study the outcome of variation in dimensional parameters of geometry on the charging and discharging characteristics (Dubey and Kumar, 2021a, 2021b). The study concludes that the reactor having lesser radial and higher longitudinal dimensions possesses better heat transfer and thus improves the charging and discharging characteristics. The energy storage capacity, discharge capacity, and storage efficiency for three cases of aspect ratio were evaluated in another analysis (Dubey and Kumar, 2022). The energy stored and released for the system was observed maximum for lower aspect ratio geometry, while the energy storage efficiency was maximum for higher aspect ratio geometry.

Several recent studies have been performed on dual metal hydride systems for thermal energy storage. Anna et al. performed the feasibility and performance study of two pairs of metal hydrides for TES applications. In one study, $NaMgH_2F$ acts as HTMH and $TiCr_{1.6}Mn_{0.2}$ acts as LTMH (D'Entremont et al., 2018). The energy storage system was found suitable, and the energy storage density was reported as 226 kWh/m^3. Next study used Mg_2FeH_6 as HTMH and Na_3AlH_6 as LTMH for a dual metal hydride system (D'Entremont. et al., 2017). The energy storage system was feasible and suitable for a temperature range of 450-500 ºC with an energy storage density of 132 kWh/m^3. This pair of metal hydrides (Mg_2FeH_6 and Na_3AlH_6) was also studied with fin arrangements for better heat transfer (Sofiene Mellouli et al., 2018). The system reported 96% energy storage efficiency with 90 kWh/m^3

energy storage density. Pair of Mg_2Ni alloy and $LaNi_5$ alloy was used in dual metal hydride based TES system. as HTMH and LTMH respectively was studied for TES applications (Malleswararao et al., 2020). The authors reported 89.4% energy efficiency with a energy storage density of 156 kWh/m^3. Some of the metal hydride systems for low temperature TES have been studied for their feasibility and performance (Choudhari and Sharma, 2020; Gambini et al., 2020; Malleswararao et al., 2022, 2021). Mg based alloys were studied and found suitable for TES applications for temperature range of 250 to 550 ºC (Bogdanović et al., 1999; Reiser et al., 2000b).

In this work, the dual metal hydride bed system with $NaMgH_2F$ as HTMH and Mg_2NiH_4 as LTMH is used for feasibility and performance analysis of the thermal energy absorption cycle. The geometric parameters such as the diameter to height ratio of metal hydride bed (Aspect Ratio) and the number of heat transfer tubes have been considered from the previously published work (Dubey and Kumar, 2022). The geometry section of the work discusses the details of the geometric parameter considered in the analysis. COMSOL Multiphysics 5.5 is used to perform the numerical analysis. The temperature, density, and heat transfer variations for the energy absorption cycle have been studied in this work.

2. Numerical Modelling

The study of TES in HTMH bed, which is coupled with LTMH bed is performed and discussed in this work. $NaMgH_2F$ is used as HTMH, which is used for TES, while Mg_2NiH_4 is used as LTMH, which stores hydrogen released from HTMH. 1 kg of HTMH is considered for the energy absorption analysis. The quantity of LTMH is calculated based on the quantity of hydrogen to handle. The geometry of the coupled metal hydride bed system is mentioned in figure 2

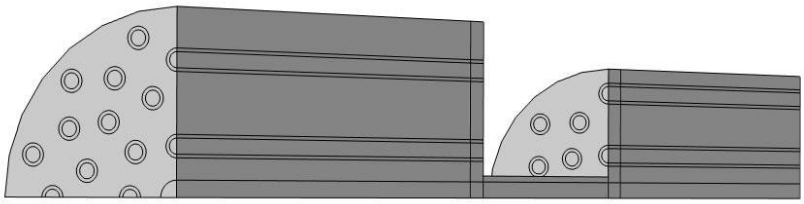

Fig 2: Coupled metal hydride bed geometry for numerical analysis

2.1. Governing Equations

The governing equations used in the numerical analysis includes mass, momentum, and energy balance equations. The energy balance equations used for different domains are represented notations in the subscript where MH bed, hydrogen gas, and heat transfer fluid are represented as “s”, “g”, and “l”, respectively. Equation (1) represents the mass balance equation for H_2 gas flowing in the porous bed, while equation (2) is the mass balance equation for the solid fraction of the porous domain. Equation (3) represents the volumetric rate of hydrogen mass desorbed. Equation (4) and (5) represents mass balance for hydrogen and HTF flow in tubes.

$$\varepsilon \frac{\partial \rho_g}{\partial t} + \nabla.\left(\rho_g u_g\right) = -S_m \quad \text{(eq. 1)}$$

$$(1-\varepsilon)\frac{\partial \rho_s}{\partial t} = S_m \quad \text{(eq. 2)}$$

$$S_m = C_a exp\left(\frac{-E_a}{RT}\right)\left(\frac{p-p_{eq}}{p_{eq}}\right) \quad \text{(eq. 3)}$$

$$\frac{\partial \rho_g}{\partial t} + \nabla.\left(\rho_g u_g\right) = 0 \quad \text{(eq. 4)}$$

$$\frac{\partial \rho_l}{\partial t} + \nabla.\left(\rho_l u_l\right) = 0 \quad \text{(eq. 5)}$$

Equation (6) represents the Brinkman equation used for the momentum balance of hydrogen flowing in the porous domain. Equation (7) and (8) represents the Navier Stokes equation used for the momentum balance of hydrogen and HTF flow in tubes.

$$\frac{\rho_g}{\varepsilon}\left(\frac{\partial u_g}{\partial t}+u_g.\frac{\nabla u_g}{\varepsilon}\right)=-\nabla p-\frac{\mu_g}{K}u_g-\frac{S_m}{\varepsilon^2}u_g+\nabla.\left[\frac{\mu_g}{\varepsilon}\left(\nabla u_g+\left(\nabla u_g\right)^T\right)-\frac{2\mu_g}{3\varepsilon}\left(\nabla.u_g\right)\right] \quad \text{(eq. 6)}$$

$$\left(\frac{\partial u_g}{\partial t}+u_g.\frac{\nabla u_g}{\varepsilon}\right)=-\nabla p+\nabla.\left[\mu_g\left(\nabla u_g+\left(\nabla u_g\right)^T\right)-\frac{2\mu_g}{3}\left(\nabla.u_g\right)\right] \quad \text{(eq. 7)}$$

$$\left(\frac{\partial u_l}{\partial t}+u_l.\frac{\nabla u_l}{\varepsilon}\right)=-\nabla p+\nabla.\left[\mu_l(\nabla u_l+(\nabla u_l)^T)-\frac{2\mu_l}{3}(\nabla.u_l)\right] \quad \text{(eq. 8)}$$

Equation (9), (13) and (14) are the energy balance equation for the porous domain, hydrogen gas and HTF flow in tubes respectively. Equation (10) and (11) expresses the relation to calculate effective thermal conductivity and effective heat capacity of metal hydride bed, which is calculated based on the average volume method. Equation (12) represents the energy source term, i.e., the volumetric energy absorption rate.

$$\left(\rho c_p\right)_{eff}\frac{\partial T}{\partial t}+\rho c_{pg}\left(u_g.\nabla T\right)=\nabla.\left(\sigma_{eff}\nabla T\right)+S_T \quad \text{(eq. 9)}$$

$$\sigma_{eff}=\varepsilon\sigma_g+(1-\varepsilon)\sigma_s \quad \text{(eq. 10)}$$

$$\left(\rho c_p\right)_{eff}=\varepsilon\left(\rho c_p\right)_g+(1-\varepsilon)\left(\rho c_p\right)_s \quad \text{(eq. 11)}$$

$$S_T=S_m(\Delta h) \quad \text{(eq. 12)}$$

$$\left(\rho_g c_{pg}\right)\left(\frac{\partial T}{\partial t}+u_g.\nabla T\right)=\nabla.\left(\sigma_g\nabla T\right) \quad \text{(eq. 13)}$$

$$\left(\rho_l c_{pl}\right)\left(\frac{\partial T}{\partial t}+u_l.\nabla T\right)=\nabla.(\sigma_l\nabla T) \quad \text{(eq. 14)}$$

The thermal and chemical properties of metal hydrides, hydrogen and heat transfer fluid are mentioned in table 1 and 2.

Table 1: Thermochemical properties of metal hydrides (D'Entremont et al., 2018; Nyamsi and Tolj, 2021; Sheppard et al., 2014)

Thermochemical Properties	**$NaMgH_2F$ (HTMH)**	**Mg_2NiH_4 (LTMH)**
Reaction rate constant (1/s)	1000000 (absorption)	175 (desorption)
Activation energy (J/mol)	102500 (absorption)	52200 (desorption)
Enthalpy of reaction (J/mol)	96800	64500
Entropy of reaction (J/mol K)	138	122.2
Specific heat capacity (J/kg K)	419	697
Gravimetric storage density (wt%)	2.5	3.6
Unsaturated density (kg/m3)	1390	3200
Saturated density (kg/m^3)	1424.75	3315.2
Thermal conductivity (W/m K)	0.5	0.2

Table 2: Geometric parameters and thermal properties of metal hydride, hydrogen, and heat transfer fluid

Thermal Properties	Value
Specific heat capacity of H_2 (J/kgK)	14539
Thermal conductivity of hydrogen (W/mK)	1
Porosity of metal hydride bed	0.5
Permeability of metal hydride bed (m^2)	10^{-8}

2.2. Assumptions

The following assumptions have been considered for the numerical analysis of energy absorption in the dual metal hydride bed system.

- Hydrogen gas is assumed as an ideal gas.
- Hydrogen gas and metal hydride bed are in thermal equilibrium.
- Metal hydride material is considered homogenous and isotropic.
- Heat transfer due to radiation is not considered inside the metal hydride bed.
- The thermal properties of metal hydride gas, hydrogen, and heat transfer fluid are considered constant.
- The outer surface of the metal hydride bed is assumed to be insulated; thus, the heat loss to the surrounding is neglected.

2.3. Geometric parameters

The dimension of the metal hydride bed is calculated based on the author's previous work (Dubey and Kumar, 2022). The geometry with an aspect ratio (ratio of diameter to height of metal hydride bed) of 0.5 has shown better heat transfer characteristics; therefore, both high and low temperature metal hydride beds are designed with an aspect ratio of 0.5. The number of heat transfer fluid tubes for both the metal hydride beds is calculated using the conclusion of the author's previous work. 1 kg of high temperature metal hydride powder is arranged in a cylindrical shape with a porosity of 0.5 and considering the aspect ratio of 0.5, the dimensions have been calculated. The low temperature metal hydride required to store the quantity of hydrogen released from high temperature metal hydride is calculated and with an aspect ratio and porosity of 0.5, the dimensions of low temperature metal hydride bed are calculated. The two metal hydride beds are connected with a tube length of 100 mm and inner and outer diameters of 9.5 and 13 mm, respectively.

Table 3: Geometric parameters of metal hydride bed

Parameter	$NaMgH_2F$ (HTMH)	Mg_2NiH_4 (LTMH)
Diameter of metal hydride bed (mm)	104	79
Height of metal hydride bed (mm)	208	158
Diameter of hydrogen supply tube (mm)	9.5	9.5
Inner diameter of heat transfer fluid tube (mm)	4.4	4.4
Outer diameter of heat transfer fluid tube (mm)	6.4	6.4
Number of heat transfer fluid tubes	44	24

2.4. Initial values and boundary conditions

Table 4: Initial values of different domains of the geometry

Initial Value	$NaMgH_2F$ (HTMH)	Mg_2NiH_4 (LTMH)
Initial temperature of metal hydride bed and HTF (K)	773	573
Initial pressure of metal hydride bed (bar)	4.64	3.18
Initial temperature of hydrogen in supply tube (K)	299	299
Initial pressure of hydrogen in supply tube (bar)	4.2	4.1
Initial pressure of heat transfer fluid (bar)	1	1
Initial density of metal hydride bed (kg/m^3)	1424.75	3200

3. Results and discussion

The results and discussion involve the analysis on the variation in temperature, density and energy absorption characteristics.

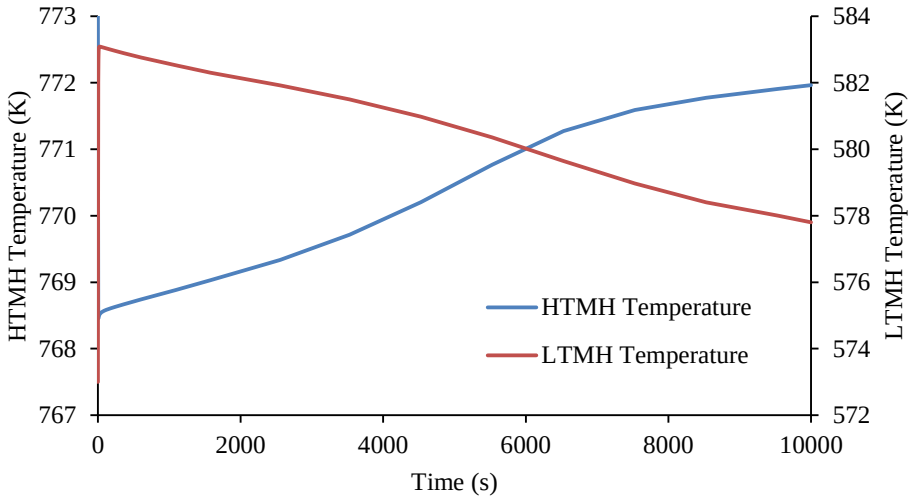

Fig. 3: Variation of average bed temperature of high and low temperature metal hydride bed with time

During energy absorption in high temperature metal hydride bed, the temperature of high temperature metal hydride bed decreases instantly because of localized energy absorption and activation energy required to initiate the endothermic chemical reaction. In low temperature metal hydride, the exothermic reaction occurs when hydrogen is absorbed, resulting in the instant increase in temperature of the metal hydride bed. After the instant variation in both beds, the average bed temperature slowly moves towards their respective steady state of the heat transfer fluid temperature, as shown in figure 3.

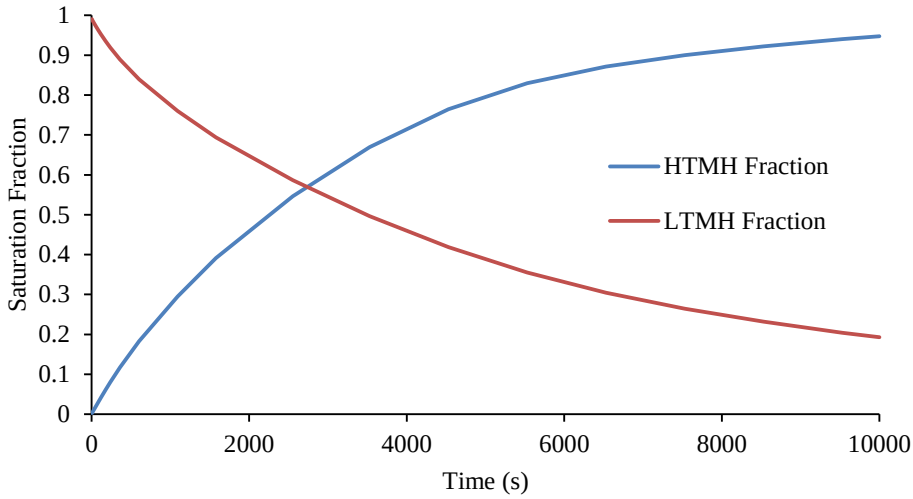

Fig. 4: Variation of saturation fraction HTMH and LTMH bed with time

The metal hydride saturation fraction has been studied for both metal hydride beds. Saturation fraction denotes the degree of energy stored in the metal hydride bed on a scale of 0 to1. 0 indicates the empty metal hydride bed, while 1 denotes the saturated metal hydride bed. The saturation fraction of the metal hydride beds are shown in figure 4.

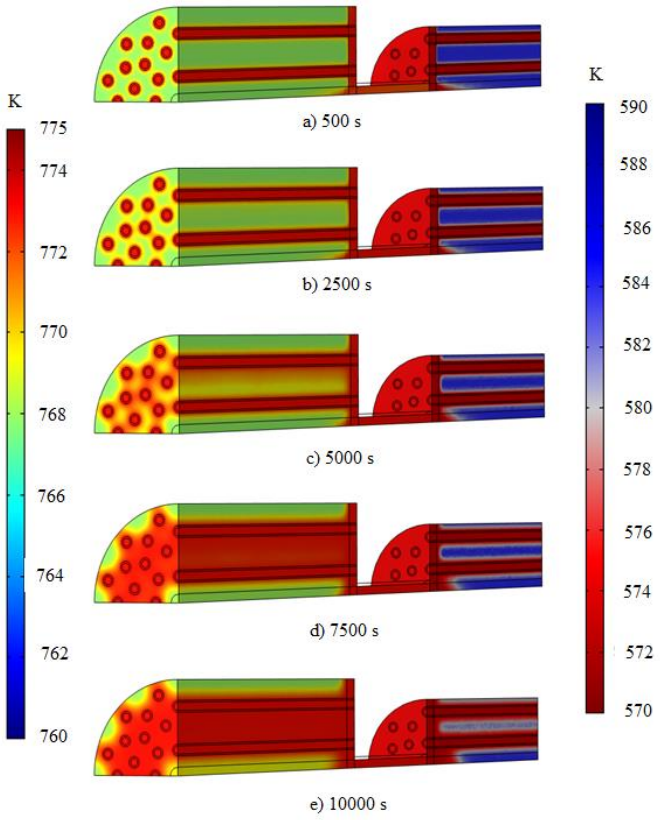

Fig. 5: Cross sectional temperature variation of geometry at different instants

The temperature and density contours of the dual metal hydride bed system at different instants are represented in figure 5 and 6, respectively. The temperature and density contours represent faster energy absorption during the initial stages, while the reaction kinetics is slower as the metal hydride beds achieve saturation.

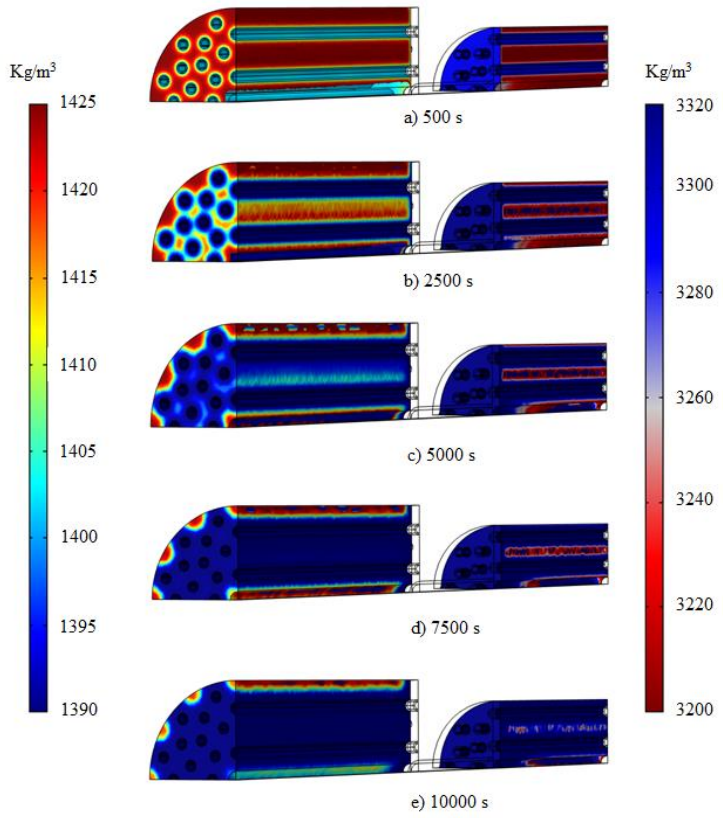

Fig. 6: Cross sectional density variation of geometry at different instants

The saturation fraction of high and low temperature metal hydride beds at different axial lengths has been studied and shown in figure 7. Three planes for both metal hydride beds at different axial lengths have been considered in the analysis. The plane closer to the connecting tube is represented as the top, while the one in the middle of the metal hydride bed is considered as middle and the third one at the opposite end is considered as the bottom,

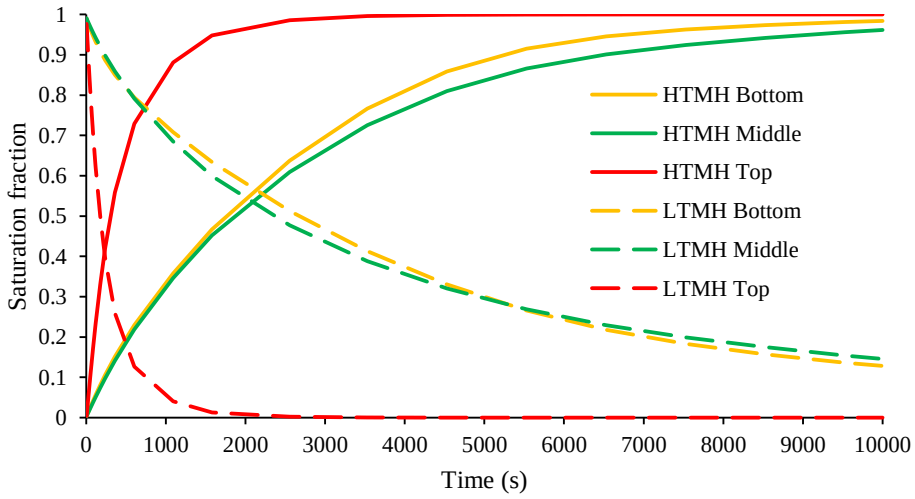

Fig. 7: Variation of saturation fraction of HTMH and LTMH bed at different axial lengths with time

The saturation fraction of the plane closer to the connecting tube is faster than the planes below it. The heat transfer fluid enters the tubes from the side of the plane at the top side and thus initially, the heat is transferred to the top plane and the plane at the top saturates in less time.

During the process of thermal energy absorption in high temperature metal hydride, a total of 256.79 kJ of thermal

energy was stored at an average bed temperature of 770 K. During the energy absorption in high temperature metal hydride, 6.93 g of hydrogen was liberated from high temperature metal hydride. The average temperature of low temperature metal hydride bed is observed as 580 K during the energy absorption process in high temperature metal hydride.

4. Conclusions

The $NaMgH_2F$ and Mg_2NiH_4 are used to study the feasibility and performance analysis of the energy absorption cycle. The two mentioned metal hydrides were found suitable for energy absorption at an average temperature of 770 K. The total thermal energy stored in the high temperature metal hydride bed is 256.79 kJ, for which 6.93 g of hydrogen was released from high temperature metal hydride. The variation of saturation fraction of the metal hydride bed with respect to time was analyzed. It is observed that the rate of energy storage in metal hydride bed is fast initially and further; the energy absorption rate decreases as the metal hydride bed moves toward saturation. The variation of saturation fraction with the axial length is also studied and the absorption rate is found to be faster for the section closer to the connecting tube.

5. Acknowledgments

The authors are thankful to Science and Engineering Research Board (SERB), Department of Science and Technology (DST), Government of India for awarding “Prime Minister Fellowship for Doctoral Research” to Mr. Sumeet Kumar Dubey in collaboration with Indian Oil Corporation Limited, Research and Development Centre and kind support from Confederation of Indian Industry (CII).

6. References

Bogdanović, B., Hofmann, H., Wessel, S., Schlichte, K., Reiser, A., Neuy, A., Spliethoff, B., 1999. Ni-doped versus undoped Mg–MgH2 materials for high temperature heat or hydrogen storage. Journal of Alloys and Compounds 292, 57–71. https://doi.org/10.1016/s0925-8388(99)00109-7

Bogdanović, B., Ritter, A., Spliethoff, B., Straßburger, K., 1995. A process steam generator based on the high temperature magnesium hydride/magnesium heat storage system. International Journal of Hydrogen Energy 20, 811–822. https://doi.org/10.1016/0360-3199(95)00012-3

Chen, X., Zhang, Z., Qi, C., Ling, X., Peng, H., 2018. State of the art on the high-temperature thermochemical energy storage systems. Energy Conversion and Management 177, 792–815. https://doi.org/10.1016/j.enconman.2018.10.011

Choudhari, M.S., Sharma, V.K., 2020. Thermodynamic simulation of hydrogen based thermochemical energy storage system. International Journal of Hydrogen Energy. https://doi.org/10.1016/j.ijhydene.2020.09.074

Choudhari, M.S., Sharma, V.K., Paswan, M., 2021. Metal hydrides for thermochemical energy storage applications. International Journal of Energy Research 1–28. https://doi.org/10.1007/978-3-319-68255-6_119

D’Entremont., A., Corgnale, C., Sulic, M., Hardy, B., Zidan, R., Motyka, T., 2017. Modeling of a thermal energy storage system based on coupled metal hydrides (magnesium iron – sodium alanate) for concentrating solar power plants. International Journal of Hydrogen Energy 42, 22518–22529. https://doi.org/10.1016/j.ijhydene.2017.04.231

D’Entremont, A., Corgnale, C., Hardy, B., Zidan, R., 2018. Simulation of high temperature thermal energy storage system based on coupled metal hydrides for solar driven steam power plants. International Journal of Hydrogen Energy 43, 817–830. https://doi.org/10.1016/j.ijhydene.2017.11.100

Dubey, S.K., Kumar, K.R., 2022. Charging and discharging analysis of thermal energy using magnesium nickel hydride based thermochemical energy storage system. Sustainable Energy Technologies and Assessments 52, 101994. https://doi.org/10.1016/j.seta.2022.101994

Dubey, S.K., Kumar, K.R., 2021a. Numerical Investigation of Thermal Energy Storage using Magnesium Nickel Hydride, in: 26th National and 4th International ISHMT-ASTFE Heat and Mass Transfer Conference. pp. 577–583. https://doi.org/10.1615/IHMTC-2021.870

Dubey, S.K., Kumar, K.R., 2021b. Numerical investigation of energy desorption from magnesium nickel hydride based thermal energy storage, in: 9th Eur. Conf. Ren. Energy Sys. Istanbul, Turkey, pp. 457–462.

Gambini, M., Stilo, T., Vellini, M., 2020. Selection of metal hydrides for a thermal energy storage device to support low-temperature concentrating solar power plants. International Journal of Hydrogen Energy 45, 28404–28425. https://doi.org/10.1016/j.ijhydene.2020.07.211

Jain, S., Dubey, S.K., Kumar, K.R., Rakshit, D., 2021a. Thermal Energy Storage for Solar Energy, in: Fundamentals and Innovations in Solar Energy. pp. 167–215. https://doi.org/10.1007/978-981-33-6456-1_9

Jain, S., Kumar, K.R., Rakshit, D., 2021b. Heat transfer augmentation in single and multiple (cascade) phase change materials based thermal energy storage : Research progress , challenges , and recommendations. Sustainable Energy Technologies and Assessments 48, 101633. https://doi.org/10.1016/j.seta.2021.101633

Liu, D., Xin-Feng, L., Bo, L., Si-quan, Z., Yan, X., 2018. Progress in thermochemical energy storage for concentrated solar power: A review. International Journal of Energy Research 42, 4546–4561. https://doi.org/10.1002/er.4183

Malleswararao, K., Aswin, N., Kumar, P., Dutta, P., Srinivasa Murthy, S., 2022. Experiments on a novel metal hydride cartridge for hydrogen storage and low temperature thermal storage. International Journal of Hydrogen Energy 1–12. https://doi.org/10.1016/j.ijhydene.2022.03.097

Malleswararao, K., Aswin, N., Murthy, S.S., Dutta, P., 2021. Studies on a dynamically coupled multifunctional metal hydride thermal battery. Journal of Alloys and Compounds 866, 158979. https://doi.org/10.1016/j.jallcom.2021.158979

Malleswararao, K., N, A., Srinivasa Murthy, S., Dutta, P., 2020. Performance prediction of a coupled metal hydride based thermal energy storage system. International Journal of Hydrogen Energy 45, 16239–16253. https://doi.org/10.1016/j.ijhydene.2020.03.251

Møller, K.T., Sheppard, D., Ravnsbæk, D.B., Buckley, C.E., Akiba, E., Li, H.W., Jensen, T.R., 2017. Complex metal hydrides for hydrogen, thermal and electrochemical energy storage. Energies 10. https://doi.org/10.3390/en10101645

Nyamsi, S.N., Tolj, I., 2021. The impact of active and passive thermal management on the energy storage efficiency of metal hydride pairs based heat storage. Energies 14. https://doi.org/10.3390/en14113006

Paskevicius, M., Sheppard, D.A., Williamson, K., Buckley, C.E., 2015. Metal hydride thermal heat storage prototype for concentrating solar thermal power. Energy 88, 469–477. https://doi.org/10.1016/j.energy.2015.05.068

Pelay, U., Luo, L., Fan, Y., Stitou, D., Rood, M., 2017. Thermal energy storage systems for concentrated solar power plants. Renewable and Sustainable Energy Reviews 79, 82–100. https://doi.org/10.1016/j.rser.2017.03.139

Ray, A.K., Rakshit, D., Ravikumar, K., 2021. High-temperature latent thermal storage system for solar power: Materials, concepts, and challenges. Cleaner Engineering and Technology 4, 100155. https://doi.org/10.1016/j.clet.2021.100155

Reilly, J.J., Wiswall, R.H., 1967. Reaction of Hydrogen with Alloys of Magnesium and Copper. Inorganic Chemistry 6, 2220–2223. https://doi.org/10.1021/ic50058a020

Reiser, A., Bogdanovic, B., Schlichte, K., 2000a. The application of Mg-based metal-hydrides as heat energy storage systems. International Journal of Hydrogen Energy 25, 425–430. https://doi.org/https://doi.org/10.1016/S0360-3199(99)00057-9.

Reiser, A., Bogdanovic, B., Schlichte, K., 2000b. The application of Mg-based metal-hydrides as heat energy storage systems. International Journal of Hydrogen Energy 25.

Sheppard, D.A., Corgnale, C., Hardy, B., Motyka, T., Zidan, R., Paskevicius, M., Buckley, C.E., 2014. Hydriding characteristics of NaMgH2F with preliminary technical and cost evaluation of magnesium-based metal hydride materials for concentrating solar power thermal storage. RSC Advances 4, 26552–26562. https://doi.org/10.1039/c4ra01682c

Sheppard, D.A., Humphries, T.D., Buckley, C.E., 2016a. Sodium-based hydrides for thermal energy applications. Applied Physics A: Materials Science and Processing 122, 1–13. https://doi.org/10.1007/s00339-016-9830-3

Sheppard, D.A., Paskevicius, M., Humphries, T.D., Felderhoff, M., Capurso, G., Bellosta von Colbe, J., Dornheim, M., Klassen, T., Ward, P.A., Teprovich, J.A., Corgnale, C., Zidan, R., Grant, D.M., Buckley, C.E., 2016b. Metal hydrides for concentrating solar thermal power energy storage. Applied Physics A: Materials Science and Processing 122, 1–15. https://doi.org/10.1007/s00339-016-9825-0

Sofiene Mellouli, Askri, F., Edacherian, A., Alqahtani, T., Algarni, S., Abdelmajid, J., Phelan, P., 2018. Performance analysis of a thermal energy storage based on paired metal hydrides for concentrating solar power plants. Applied Thermal Engineering 144, 1017–1029. https://doi.org/.1037//0033-2909.I26.1.78

Sunku Prasad, J., Muthukumar, P., Desai, F., Basu, D.N., Rahman, M.M., 2019. A critical review of high-temperature reversible thermochemical energy storage systems. Applied Energy 254, 113733. https://doi.org/10.1016/j.apenergy.2019.113733

Appendix: Units and Symbols

Table 1: Symbols for materials properties

Quantity	Symbol	Unit
Specific heat	c	J kg^{-1} K^{-1}
Rate constant	C	s^{-1}
Activation energy	E	J kg^{-1}
Thermal conductivity	σ	W m^{-1} K^{-1}
Permeability	K	m^2
Porosity	ε	
Viscosity	μ	kg m^{-1} s^{-1}
Reaction enthalpy	Δh	J mol^{-1}
Reaction entropy	Δs	J mol^{-1} K^{-1}
Heat transfer coefficient	h	W m^{-2} K^{-1}
Density	ρ	kg m^{-3}

Table 2: Symbols for miscellaneous quantities

Quantity	Symbol	Unit
Pressure	p	bar
Temperature	T	K
Velocity	u	m s^{-1}
Thermal conductivity	σ	W m^{-1} K^{-1}
Time	t	s

Table 3: Symbols for chemical compounds

Chemical element	Symbol
Magnesium	Mg
Nickel	Ni
Sodium	Na
Hydrogen	H
Fluorine	F
Lanthanum	La
Aluminium	Al
Iron (Ferrous)	Fe
Titanium	Ti
Chromium	Cr
Manganese	Mn
Cobalt	Co

Table 4: Subscripts

Description	Symbol
Metal hydride (solid)	s
Hydrogen (gas)	g
Heat transfer fluid	l
absorption	a
mass	m
Thermal energy	T